Inorg. Chem. **2004**, *43*, 198–205

Synthesis and Structures of New Pyromellitate Coordination Polymers with Piperazine as a Ligand

S. V. Ganesan and Srinivasan Natarajan*

Framework Solids Laboratory, Chemistry and Physics of Materials Unit, Jawaharlal Nehru Centre for Advanced Scientific Research, Jakkur P.O., Bangalore 560 064, India

Received July 17, 2003

Two new coordination polymers of the pyromellitic acid, $[Zn_2(H_2O)(C_{10}H_2O_8)(C_4N_2H_8)]_\infty$, **I**, and $[Cd_4(H_2O)_2(C_{10}H_2O_8)_2(C_4N_2H_8)_3]_\infty$, **II**, have been prepared employing hydrothermal methods in the presence of piperazine. The structures have three-dimensional connectivity involving both the carboxylate and the amine molecule. The amine molecule acts as a ligand connecting two different metal centers giving rise to a simple dimer in **I**, and a two-dimensional layer structure in **II**. There are two types of pyromellitates in **I** and only one type in **II**. Of the two types of acids in **I**, acid-1 has all the oxygen atoms connected to Zn with monodendate connectivity and acid-2 has only four monodendate connectivity and possesses four terminal C–O linkage. In **II**, two of the carboxylates have bidendate connectivity and the other two have monodendate connectivity and possess one terminal C–O bond. The projection of the bound amine molecules, in **II**, into the large elliptical channels is noteworthy. These amine molecules may be amenable for chemical manipulations. Both the coordination polymers exhibit photoluminescence at room temperature, the main emission being at 380 and 410 nm, respectively, for **I** and **II**, which is due to the ligand-to-metal charger transfer (LMCT).

Introduction

Benzene carboxylate compounds are of topical interest. Extensive investigations by many researchers have given rise to a large number of coordination polymers with interesting structural, physical and chemical properties.[1] Of the many benzene carboxylate compounds that have been prepared and characterized, those of the pyromellitic acid have been of interest to us.[2−13] The variations in the binding modes of the four acid functional groups combined with the coordination preferences of the metal ions are important in giving rise to the many different coordination polymers. We have been focusing our attention on the preparation of benzene carboyxlate coordination polymers in the presence of organic amine molecules. During the course of such investigations, we have now isolated two new coordination polymers of the pyromellitic acid (1,2,4,5-benzenetetracaroxylic acid, BTEC), $[Zn_2(H_2O)(C_{10}H_2O_8)(C_4N_2H_8)]_\infty$, **I**, and $[Cd_4(H_2O)_2(C_{10}H_2O_8)_2(C_4N_2H_8)_3]_\infty$, **II**, in the presence of piperazine, employing hydrothermal methods. Both **I** and **II** have three-dimensional structures, and the piperazine molecule acts as a ligand to the metal ions. The projection of one of the bound amine molecules into the channels in **II** gives rise to the possibility of chemical manipulation. In this paper, we describe the synthesis, structure, and characterization of both compounds.

* Corresponding author. E-mail: raj@jncasr.ac.in. Fax: +91-80-846-2766; +91-80-856-6581.

(1) Rao, C. N. R.; Natarajan, S.; Vaidhyanathan, R. *Angew. Chem., Int. Ed.* **2004**, in press.
(2) Cao, R.; Shi, Q.; Sun, D.; Hong, M.; Bi, W.; Zhao, Y. *Inorg. Chem.* **2002**, *41*, 6161.
(3) Chu, D. Q.; Xu, J. Q.; Duan, L. M.; Wang, T. G.; Tang, A. Q.; Ye, L. *Eur. J. Inorg. Chem.* **2001**, 1135.
(4) Senselme, M.; Riou-Cavellec, M.; Ferey, G. *Solid State Sci.* **2002**, *4*, 1419.
(5) Kim, J. C.; Lough, A. J.; Kim, H. *Inorg. Chem. Commun.* **2002**, *5*, 771.
(6) Li, Y.; Zhang, H.; Wang, E.; Hao, N.; Hu, C.; Yan, Y.; Hall, D. *New J. Chem.* **2002**, *26*, 1619.
(7) Chiang, R. K.; Chuang, N. T.; Wur, C. S.; Chong, M. F.; Lin, C. R. *J. Solid State Chem.* **2002**, *166*, 158.
(8) Gutschke, S. O. H.; Price, D. J.; Powell, A. K.; Wood, P. T. *Eur. J. Inorg. Chem.* **2001**, 2739.
(9) Cheng, D.; Khan, M. A.; Houser, R. P. *J. Chem. Soc., Dalton Trans.* **2002**, 4555.
(10) Murugavel, R.; Krishnamurthy, D.; Sathiyendiran, M. *J. Chem. Soc., Dalton Trans.* **2002**, 34.
(11) Barthelet, K.; Riou, D.; Nogues, M.; Ferey, G. *Inorg. Chem.* **2003**, *42*, 1739.
(12) Cao, R.; Sun, D.; Liang, Y.; Hong, M.; Tatsumi, K.; Shi, Q. *Inorg. Chem.* **2002**, *41*, 2087.
(13) Sanselme, M.; Greneche, J. M.; Riou-Cavellec, M.; Ferey, G. *Chem. Commun.* **2002**, 2172.

10.1021/ic034836p CCC: $27.50
Published on Web 12/03/2003

Table 1. Crystal Data and Structure Refinement Parameters for $[Zn_2(H_2O)(C_{10}H_2O_8)(C_4N_2H_8)]_\infty$, **I**, and $[Cd_4(H_2O)_2(C_{10}H_2O_8)_2(C_4N_2H_8)_3]_\infty$, **II**

structure parameter	**I**	**II**
empirical formula	$C_{14}H_{12}N_2O_9Zn_2$	$C_{16}H_{16}N_3O_9Cd_2$
fw	483.04	619.12
cryst syst	monoclinic	monoclinic
space group	$P2_1/n$ (no. 14)	$P2_1/n$ (no. 14)
cryst size (mm)	0.24 × 0.16 × 0.16	0.24 × 0.12 × 0.12
a (Å)	8.6035(1)	6.3028(3)
b (Å)	11.5305(3)	18.0250(8)
c (Å)	15.5628(4)	16.0261(7)
β (deg)	96.757(2)	93.975(1)
vol (Å^3)	1533.15(6)	1816.31(14)
Z	4	4
ρ_{calc} (g cm^{-3})	2.093	2.264
μ (mm^{-1})	3.188	2.402
θ range (deg)	2.2−23.3	1.70−23.22
tot. no of data collcd	6292	7434
no. of unique data	2201	2580
refinement method	full-matrix least-squares on $\|F^2\|$	full-matrix least-squares on $\|F^2\|$
R_{merg}	0.047	0.0246
R indexes [$I > 2\sigma(I)$]	$R_1 = 0.0374$,[a] $wR_2 = 0.0793$[b]	$R_1 = 0.0240$,[a] $wR_2 = 0.0589$[b]
R (all data)	$R_1 = 0.0603$, $wR_2 = 0.0892$	$R_1 = 0.0293$, $wR_2 = 0.0610$
goodness of fit (S_{obsd})	1.059	1.042
no. of variables	252	279
largest diff map hole and peak, e Å^{-3}	−0.538 and +0.657	−0.729 and +0.713

[a] $R_1 = \sum ||F_0| - |F_c||/\sum |F_0|$. [b] $wR_2 = \{\sum[w(F_0^2 - F_c^2)^2]/\sum[w(F_0^2)^2]\}^{1/2}$. $w = 1/[\sigma^2(F_0)^2 + (aP)^2 + bP]$, $P = [\max(F_0^2,0) + 2(F_c)^2]/3$, where $a = 0.0310$ and $b = 3.5915$ for **I** and $a = 0.0312$ and $b = 2.0546$ for **II**.

Experimental Section

Synthesis of $[Zn_2(H_2O)(C_{10}H_2O_8)(C_4N_2H_8)]_\infty$, I, and $[Cd_4(H_2O)_2(C_{10}H_2O_8)_2(C_4N_2H_8)_3]_\infty$, II. The two coordination polymers **I** and **II** were synthesized employing hydrothermal methods in the presence piperazine. In a typical synthesis, for **I**, 0.08 g of ZnO was dispersed in 2 mL of water. To this, 0.499 g of piperazine (PIP) and 0.66 mL of 1,4-bis(3-aminopropyl)piperazine (APPIP) were added under continuous stirring. Finally, 0.499 g of pyromellitic acid (BTEC) was added, and the mixture was homogenized at room temperature for about 1 h. The final reaction mixture with the composition, ZnO:2BTEC:5.9PIP:3.2APPIP:$113H_2O$, was sealed in a PTFE-lined stainless steel autoclave (23 mL capacity) and heated at 180 °C for 92 h followed by at 200 °C for 115 h. The resulting product, containing large quantities of colorless hexagonal rodlike single crystals, was filtered, washed with deionized water, and dried at ambient conditions. The yield of the product was ∼70% based on Zn. The role of APPIP in the synthesis of **I** is still not clear. Our efforts to prepare **I** in the absence of it and by increasing the corresponding concentration of PIP did not give **I**. For **II**, a composition of cadmium sulfate, pyromellitic acid, piperazine, and water were taken in the ratio 1:1:10:130 and heated at 180 °C for 72 h to result in large quantities of hexagonal rodlike single crystals (yield 80% based on Cd). The initial and final pH of the reaction mixture was ∼5 for **I** and ∼10.5 for **II**.

Single-Crystal Structure Determination. A suitable colorless single crystal of each compound was carefully selected under a polarizing microscope and glued to a thin glass fiber with cyanoacrylate (superglue) adhesive. Crystal structure determination by X-ray diffraction was performed on a Siemens SMART-CCD diffractometer equipped with a normal focus, 2.4 kW sealed tube X-ray source (Mo Kα radiation, $\lambda = 0.710\ 73$ Å) operating at 50 kV and 40 mA. A hemisphere of intensity data was collected at room temperature in 1321 frames with ω scans (width of 0.30° and exposure time of 10 s per frame) in the 2θ range 3−46.5°. Pertinent experimental details for the structure determinations of **I** and **II** are presented in Table 1.

An absorption correction was applied using the SADABS program (0.707 956, 1.000 000 for **I** and 0.814 065, 1.000 000 for **II**).[14] The structures were solved by direct methods, and in each case, a sufficient fragment of the structure was revealed to enable the remainder of the non-hydrogen atoms to be located from difference Fourier maps and the refinements to proceed to $R <$ 10%. All the hydrogen positions for both the compounds were initially located in the difference map, and for the final refinement the hydrogen atoms were placed geometrically and held in the riding mode. The last cycles of refinement included atomic positions for all the atoms, anisotropic thermal parameters for all the non-hydrogen atoms, and isotropic thermal parameters for all the hydrogen atoms. Full-matrix least-squares refinement against $|F^2|$ was carried out using the SHELXTL-PLUS[15] suite of programs. Details of the final refinement are given in Table 1. The selected bond distances and angles are given in Table 2 for **I** and in Table 3 for **II**.

Results

Initial Characterization. The compounds **I** and **II** were characterized by elemental analysis, powder X-ray diffraction (XRD), TGA, IR, NMR, and photoluminescence studies. Anal. Calcd for **I**: C, 33.96; N, 5.8; H, 2.5. Found: C, 34.7; N, 6.05; H, 2.6. Calcd for **II**: C, 31.04; N, 6.78; H, 2.60. Found: C, 31.2; N, 6.83; H, 2.7. The powder XRD patterns were recorded on crushed single crystals in the 2θ range 5−50° using Cu Kα radiation (Rich-Seifert, 3000TT). The XRD patterns indicated that the products were new materials; the patterns were entirely consistent with the structures determined using the single-crystal X-ray diffraction. As a representative example, the powder XRD pattern along with the simulated one for **II** is given in Figure 1.

Thermogravimetric analysis (TGA) has been carried out (Mettler-Toledo, TG850) in nitrogen atmosphere

(14) Sheldrick, G. M. *SADABS Siemens Area Detector Absorption Correction* Program; University of Gottingen: Gottingen, Germany, 1994.
(15) Sheldrick, G. M. *SHELX-97 Program for Crystal Structure Solution and* Refinement; University of Gottingen, Gottingen, Germany, 1997.

Table 2. Selected Bond Distances and Angles in **I**, $[Zn_2(H_2O)(C_{10}H_2O_8)(C_4N_2H_8)]_\infty$[a]

bond	distance (Å)	bond	distance (Å)
Zn(1)−O(1)	1.998(4)	N(1)−C(1)	1.485(7)
Zn(1)−O(2)	2.000(4)	N(1)−C(2)	1.470(7)
Zn(1)−O(3)	2.063(4)	N(2)−C(3)	1.483(7)
Zn(1)−O(4)	2.264(4)	N(2)−C(4)	1.492(7)
Zn(1)−N(1)	2.074(4)	C(1)−C(4)#2	1.519(8)
Zn(2)−O(7)	1.964(4)	C(2)−C(3)#2	1.514(8)
Zn(2)−O(5)	1.972(4)	C(11)−C(12)	1.518(7)
Zn(2)−O(6)	1.985(4)	C(12)−C(14)#4	1.386(7)
Zn(2)−N(2)	2.044(4)	C(12)−C(13)	1.404(8)
O(1)−C(11)	1.286(7)	C(13)−C(14)	1.393(7)
O(2)−C(20)	1.272(7)	C(13)−C(20)#5	1.501(8)
O(3)−C(18)	1.253(7)	C(15)−C(16)	1.518(7)
O(4)−C(15)	1.227(6)	C(16)−C(17)	1.410(7)
O(5)−C(15)#1	1.258(6)	C(18)−C(17)	1.522(7)
O(7)−C(18)	1.252(7)	C(20)−C(13)#6	1.501(8)
O(8)−C(11)	1.229(6)	C(19)−C(17)	1.380(7)
O(9)−C(20)	1.247(6)	C(19)−C(16)#7	1.385(7)

angle	amplitude (deg)	angle	amplitude (deg)
O(1)−Zn(1)−O(2)	106.6(2)	O(7)−Zn(2)−N(2)	116.0(2)
O(1)−Zn(1)−O(3)	129.2(2)	O(5)−Zn(2)−N(2)	107.4(2)
O(2)−Zn(1)−O(3)	89.1(2)	O(6)−Zn(2)−N(2)	107.8(2)
O(1)−Zn(1)−N(1)	114.7(2)	C(11)−O(1)−Zn(1)	118.0(3)
O(2)−Zn(1)−N(1)	95.0(2)	C(20)−O(2)−Zn(1)	123.2(4)
O(3)−Zn(1)−N(1)	111.5(2)	C(18)−O(3)−Zn(1)	131.9(4)
O(1)−Zn(1)−O(4)	89.9(2)	C(15)−O(4)−Zn(1)	130.5(4)
O(2)−Zn(1)−O(4)	162.8(2)	C(15)#1−O(5)−Zn(2)	119.8(4)
O(3)−Zn(1)−O(4)	76.5(2)	C(18)−O(7)−Zn(2)	114.2(4)
N(1)−Zn(1)−O(4)	81.9(2)	O(8)−C(11)−O(1)	124.6(5)
O(7)−Zn(2)−O(5)	116.6(2)	O(4)−C(15)−O(5)#1	123.4(5)
O(7)−Zn(2)−O(6)	105.1(2)	O(9)−C(20)−O(2)	124.8(5)
O(5)−Zn(2)−O(6)	102.8(2)	O(7)−C(18)−O(3)	123.4(5)

[a] Symmetry transformations used to generate equivalent atoms: #1, $-x$, $-y$, $-z+2$; #2, $-x-1/2$, $y+1/2$, $-z+3/2$; #4, $-x+1$, $-y+1$, $-z+2$; #5, $-x+1/2$, $y+1/2$, $-z+3/2$; #6, $-x+1/2$, $y-1/2$, $-z+3/2$; #7, $-x+1$, $-y$, $-z+2$.

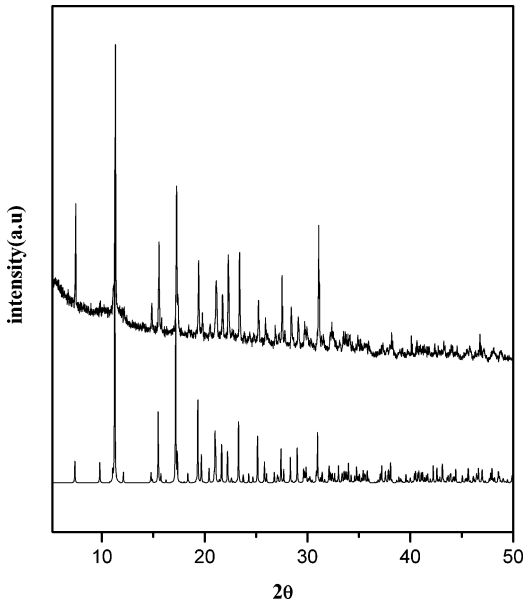

Figure 1. Powder X-ray diffraction (Cu Kα) pattern along with a simulated one for $[Cd_4(H_2O)_2(C_{10}H_2O_8)_2(C_4N_2H_8)_3]_\infty$, **II**.

(flow rate = 50 mL/min) in the temperature range 25−700 °C (heating rate = 2 °C/min). The studies show similar results for both compounds.Total weight losses of 75% and 63.2% have been observed in the case of **I** and **II**,

Table 3. Selected Bond Distances and Angles in **II**, $[Cd_4(H_2O)_2(C_{10}H_2O_8)_2(C_4N_2H_8)_3]_\infty$[a]

bond	distance (Å)	bond	distance (Å)
Cd(1)−O(1)	2.246(3)	C(1)−C(2)	1.505(5)
Cd(1)−O(2)	2.287(3)	C(2)−C(3)	1.408(6)
Cd(1)−N(3)	2.293(3)	C(3)−C(4)	1.398(5)
Cd(1)−O(3)	2.429(3)	C(4)−C(5)	1.395(5)
Cd(1)−N(1)	2.440(3)	C(5)−C(6)	1.403(5)
Cd(1)−O(4)	2.458(3)	C(6)−C(7)	1.388(5)
Cd(2)−O(5)	2.279(3)	C(2)−C(7)	1.390(5)
Cd(2)−O(6)	2.288(3)	C(3)−C(8)	1.517(5)
Cd(2)−OW	2.314(3)	C(5)−C(31)#2	1.511(5)
Cd(2)−N(2)	2.325(3)	C(6)−C(21)#3	1.508(5)
Cd(2)−O(7)	2.385(3)	N(1)−C(11)	1.490(5)
Cd(2)−O(4)	2.487(3)	N(1)−C(12)	1.488(5)
O(1)−C(31)	1.254(5)	C(11)−C(52)#4	1.516(6)
O(2)−C(1)	1.269(5)	C(12)−C(51)#4	1.511(6)
O(3)−C(1)	1.258(5)	N(3)−C(52)	1.479(5)
O(4)−C(8)#1	1.260(5)	N(3)−C(51)	1.500(5)
O(5)−C(31)	1.246(5)	N(2)−C(41)	1.484(5)
O(6)−C(21)	1.251(4)	N(2)−C(42)#5	1.491(5)
O(7)−C(8)#1	1.266(5)	C(41)−C(42)	1.499(6)
O(8)−C(21)	1.260(5)		

angle	amplitude (deg)	angle	amplitude (deg)
O(1)−Cd(1)−O(2)	152.70(10)	O(6)−Cd(2)−O(7)	94.11(9)
O(1)−Cd(1)−N(3)	90.95(11)	OW−Cd(2)−O(7)	104.11(10)
O(2)−Cd(1)−N(3)	116.27(11)	N(2)−Cd(2)−O(7)	90.47(10)
O(1)−Cd(1)−O(3)	97.02(9)	O(5)−Cd(2)−O(4)	109.79(9)
O(2)−Cd(1)−O(3)	56.09(9)	O(6)−Cd(2)−O(4)	83.38(9)
N(3)−Cd(1)−O(3)	170.53(10)	OW−Cd(2)−O(4)	154.50(10)
O(1)−Cd(1)−N(1)	93.21(11)	N(2)−Cd(2)−O(4)	97.20(10)
O(2)−Cd(1)−N(1)	87.49(11)	O(7)−Cd(2)−O(4)	53.70(9)
N(3)−Cd(1)−N(1)	93.36(11)	C(31)−O(1)−Cd(1)	137.5(3)
O(3)−Cd(1)−N(1)	81.14(10)	C(1)−O(2)−Cd(1)	93.2(2)
O(1)−Cd(1)−O(4)	90.89(10)	C(1)−O(3)−Cd(1)	87.0(2)
O(2)−Cd(1)−O(4)	81.63(10)	C(8)#1−O(4)−Cd(1)	155.3(2)
N(3)−Cd(1)−O(4)	102.50(11)	C(8)#1−O(4)−Cd(2)	90.2(2)
O(3)−Cd(1)−O(4)	82.55(9)	Cd(1)−O(4)−Cd(2)	103.89(10)
N(1)−Cd(1)−O(4)	163.55(10)	C(31)−O(5)−Cd(2)	122.0(2)
O(5)−Cd(2)−O(6)	90.46(10)	C(21)−O(6)−Cd(2)	121.6(2)
O(5)−Cd(2)-OW	93.54(10)	C(8)#1−O(7)−Cd(2)	94.8(2)
O(6)−Cd(2)-OW	86.35(10)	O(3)−C(1)−O(2)	123.0(3)
O(5)−Cd(2)−N(2)	84.36(11)	O(4)#4−C(8)−O(7)#4	121.4(3)
O(6)−Cd(2)−N(2)	174.68(10)	O(6)−C(21)−O(8)	126.1(3)
OW−Cd(2)−N(2)	95.18(11)	O(5)−C(31)−O(1)	126.0(4)
O(5)−Cd(2)−O(7)	162.00(10)		

[a] Symmetry transformations used to generate equivalent atoms: #1, $x+1$, y, z; #2, $-x-1/2$, $y+1/2$, $-z+1/2$; #3, $-x+1/2$, $y+1/2$, $-z+1/2$; #4, $x-1$, y, z; #5, $-x$, $-y+1$, $-z$.

respectively. The weight loss corresponds to the loss of bound water molecules, the amine, and the carboyxlate anions. The calcined sample was crystalline, and the powder XRD lines matches well with the corresponding pure oxides in both the cases.

Infrared (IR) spectroscopic studies have been carried out in the mid-IR region as a KBr pellet (Bruker IFS-66v). The spectra indicated characteristic sharp lines with almost similar bands. Minor variations in the bands have been noticed between the two compounds. The observed bands for **I** are 3475 cm^{-1} = lattice water, 3262 cm^{-1} = ν_s(OH), 3177 cm^{-1} = $\nu_{as}(C-H)_{aromatic}$, 2911 cm^{-1} = $\nu_{as}(C-H)_{piperazine}$, 1622 cm^{-1} = $\nu_{as}(C=O)$, 1491 = $(C-C)_{skeletal}$, 1430 and 1359 cm^{-1} = δ(OH), 1325 cm^{-1} = δ(CO), 1279 cm^{-1} = $\delta(CH_{aromatic})_{in-plane}$, 1012 cm^{-1} = ν(C−N), and 887 and 810 cm^{-1} = $\delta(CH_{aromatic})_{out-of-plane}$. The observed bands for **II** are 3476 cm^{-1} = lattice water, 3232 cm^{-1} = ν_s(OH), 3164

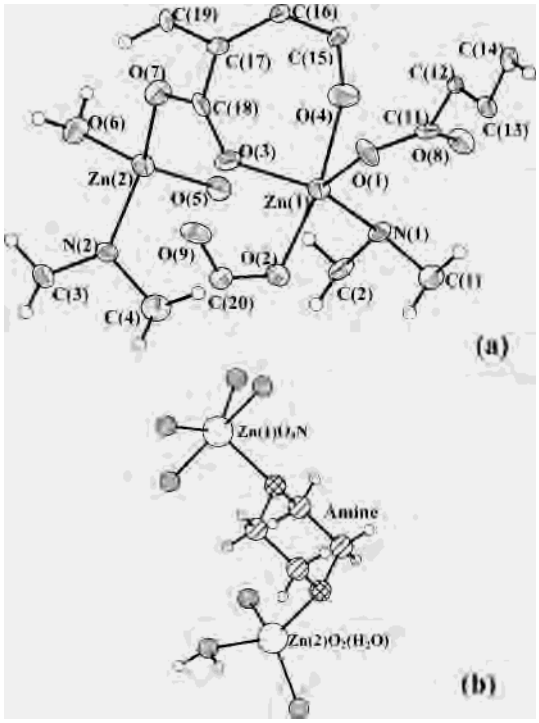

Figure 2. (a) ORTEP diagram showing the asymmetric unit in $[Zn_2(H_2O)(C_{10}H_2O_8)(C_4N_2H_8)]_\infty$, **I**. Thermal ellipsoids are given at 50% probability. (b) Connectivity between Zn and the piperazine molecule.

$cm^{-1} = \nu_{as}(C-H)_{aromatic}$, 2936 $cm^{-1} = \nu_{as}(C-H)_{piperazine}$, 1568 $cm^{-1} = \nu_{as}(C{=}O)$, 1538 $= (C-C)_{skeletal}$, 1429 and 1384 $cm^{-1} = \delta(OH)$, 1295 $cm^{-1} = \delta(CO)$, 1282 $cm^{-1} = \delta(CH_{aromatic})_{in-plane}$, 1216 $cm^{-1} = \nu(C-N)$, and 863 and 809 $cm^{-1} = \delta(CH_{aromatic})_{out-of-plane}$.

Solid-state nuclear magnetic resonance (NMR) experiments were performed on a Bruker DSX 300 spectrometer operating at 7.4 T with a resonance frequency of 75.47 MHz for ^{13}C. A Bruker 4 mm CPMAS probe was used for all experiments. The ^{13}C MAS spectra were recorded using standard cross-polarization (CP) procedures, employing magic angle spinning (MAS) frequency of 1509 Hz. In a typical experiment, RF fields of 6.5 kHz were used for ^{13}C. Chemical shifts are reported relative to $CDCl_3$ as an external standard.

Structure of $[Zn_2(H_2O)(C_{10}H_2O_8)(C_4N_2H_8)]_\infty$, I. The structure of **I** has 26 non-hydrogen atoms in the asymmetric unit, of which there are two crystallographically distinct Zn atoms (Figure 2a). While Zn(2) is tetrahedrally coordinated to three-oxygen atoms and a nitrogen atom, Zn(1) has a distorted trigonal-bipyramidal coordination with four oxygen atoms and a nitrogen atom. The Zn−O/N distances are in the range 1.964(4)−2.264(4) Å (av. 2.040 Å). The Zn(2)−O(3) distance (2.852 Å) show some weak interaction between the zinc and the oxygen atoms, which may be viewed as semi-chelation coordination mode.[16] Thus, one can describe the coordination environment of Zn(2) atom also as a distorted trigonal-bipyramidal. The O/N−Zn−O/N bond angles are in the range 76.5(20−162.8(2)° (av. 107.1°). Zn(1) and Zn(2) atoms are connected together through a piperazine molecule (Figure 2b) and Zn(2) has a terminal Zn−O linkage which is formally a water molecule. The Zn atoms are connected to the pyromellitic acid through Zn−O−C bonds. Both the Zn atoms make three Zn−O−C bonds with an average bond angle of 122.9°. The connectivity between the pyromellitic acid and the Zn atoms, on the other hand, show distinct differences. There are two types of pyromellitic acids present in the structure. The benzene ring of acid-1 is formed by the carbon atoms C(16), C(17) and C(19), with C(19) occupying the crystallogrphic 2-fold axis with a site-occupancy (SOF) of 0.5 and C(15) and C(18) forming the two carboxylate groups. The benzene ring of acid-2 is formed by C(12), C(13) and C(14), with C(14) occupying the crystallographic 2-fold axis with a site-occupancy (SOF) of 0.5 and C(11) and C(20) forming the two carboxylate groups. While acid-1 connects two Zn(1) and four Zn(2) atoms through all the eight C−O oxygen atoms (Figure 3a), acid-2 connects four Zn(1) only through four of its oxygen atoms and possesses four C−O terminal bonds (Figure 3b). Thus, acid-1 has all eight oxygen atoms with monodendate connectivity and acid-2 has monodendate connectivity only with respect to four oxygen atoms. The C−O bond distances are in the range 1.227(6)−1.286(7) Å (av. 1.253 Å) and O−C−O bond angles have an average value of 124.1°. These values are in the range expected for this type of bonding. The planar aromatic C−C and the

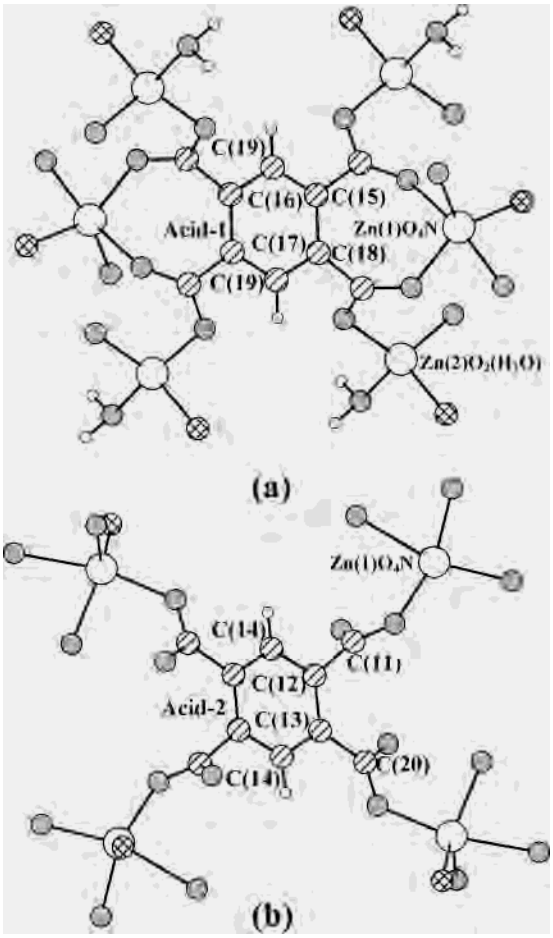

Figure 3. (a) Connectivity between the Zn and acid-1 (see text). (b) Connectivity between the Zn and acid-2 (see text).

(16) Guilera, G.; Steed, J. W. *Chem. Commun.* **1999**, 1563.

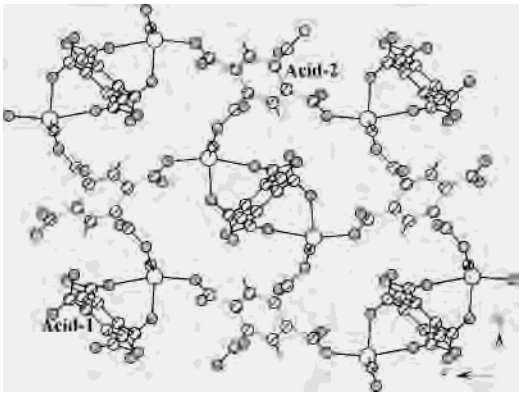

Figure 4. Structure of $[Zn_2(H_2O)(C_{10}H_2O_8)(C_4N_2H_8)]_\infty$, **I**, in the *bc* plane showing the two different acids. The bridging amine molecules are not shown for clarity.

Table 4. Important Hydrogen Bond Interactions in $[Zn_2(H_2O)(C_{10}H_2O_8)(C_4N_2H_8)]_\infty$, **I**, and $[Cd_4(H_2O)_2(C_{10}H_2O_8)_2(C_4N_2H_8)_3]_\infty$, **II**

D−H···A moiety	D−H	H···A	D···A	D−H···A
		I		
O(6)−H(11)···O(9)	0.95	1.83	2.690(6)	150
O(6)−H(12)···O(8)	0.95	1.75	2.663(6)	159
C(1)−H(1)−O(5)	0.97	2.26	3.099(8)	144
C(2)−H(1)···O(5)	0.97	2.50	3.446(7)	165
C(3)−H(5)···O(9)	0.97	2.48	3.305(7)	143
		II		
O(w)−H(15)···O(7)	0.94	1.85	2.779(4)	166
O(w)−H(16)···O(8)	0.95	1.72	2.634(4)	159
C(11)−H(4)···O(2)	0.97	2.59	3.402(5)	142
C(41)−H(8)···O(w)	0.97	2.33	3.205(5)	150

terminal C−C bond distances are also in the range expected. Bond valence sum calculations[17] clearly indicate that the valence states of the Zn, C and O atoms as +2, +4, and −2, respectively.

The structure of **I** consists of linkages between $Zn(1)O_4N$ and $Zn(2)O_2(H_2O)N$, and the two types of acids, in addition to the amine molecule, giving rise to a three-dimensionally extended coordination polymer. Though, zinc pyromellitates and other benzene carboxylates have been prepared before, to our knowledge, this is the first time a three-dimensional structure has been obtained involving a simple nitrogen donor amine (piperazine) and the acid. The observed differences between the monodendate connectivity between the two acids are also reflected in the structure. The connectivity between the Zn atoms and the two acids in the *bc* plane are shown in Figure 4. As can be noted, the structure packs in such a way that there are no significant $\pi-\pi$ interactions. Medium-strength hydrogen-bond interactions have been observed involving the hydrogen atoms of the water and the piperazine molecule with the oxygen atoms. The important hydrogen-bond interactions have been listed in Table 4.

Structure of $[Cd_4(H_2O)_2(C_{10}H_2O_8)_2(C_4N_2H_8)_3]_\infty$, II. The structure of **II** has 30 non-hydrogen atoms in the asymmetric unit, of which there are two crystallographically distinct Cd atoms (Figure 5a). Both the cadmium atoms have a distorted octahedral environment with oxygen and nitrogen atoms. While Cd(1) is coordinated to four oxygen and two nitrogen

(17) Brown, I. D.; Altermatt, D. *Acta Crystallogr. B* **1985**, *41*, 244.

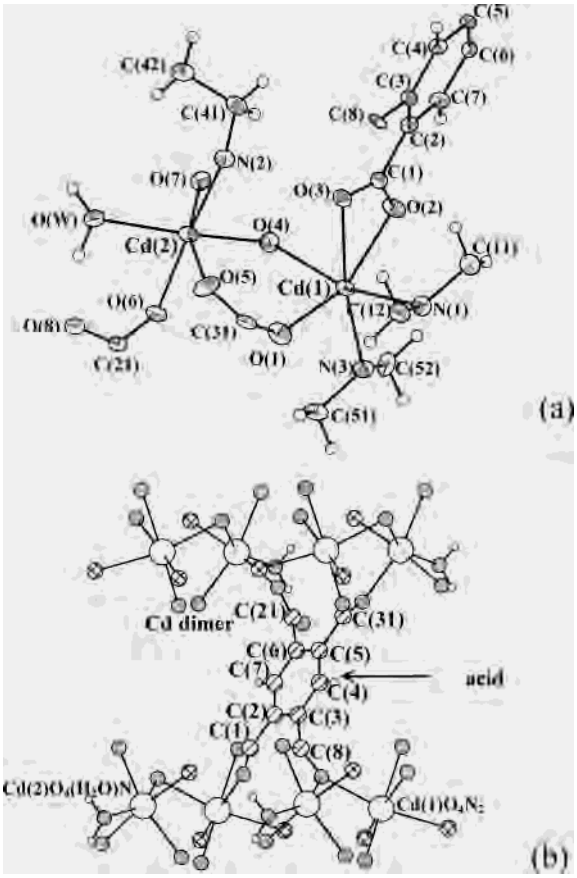

Figure 5. (a) ORTEP diagram showing the asymmetric unit in $[Cd_4(H_2O)_2(C_{10}H_2O_8)_2(C_4N_2H_8)_3]_\infty$, **II**. Thermal ellipsoids are given at 50% probability. (b) Connectivity between Cd dimers and the pyromellitic acid.

atoms, Cd(2) is coordinated with five oxygen and one nitrogen atoms with Cd−O/N distances in the range 2.246(3)−2.487(3) Å (av. 2.353 Å). The O/N−Cd−O/N bond angles are in the range 53.70(9)−174.68(10)° (av. 104.5°). The cadmium atoms, $Cd(1)O_4N_2$ and $Cd(2)O_4(H_2O)N$, are connected together through a single oxygen atom, O(4), giving rise to a $Cd_2O_9N_3$ dimer. The Cd atoms are connected to the pyromellitic acid through Cd−O−C bonds. Both the Cd atoms make four Cd−O−C bonds with an average bond angle of 112.7°. The remaining two vertexes of the Cd−O/N octahedra correspond to two Cd−N linkages for Cd(1) and to a terminal Cd−O bond and a Cd−N linkage for Cd-(2). The terminal Cd(2)−O(w) bond is formally a water molecule. Unlike **I**, there is only one type of connectivity between the pyromellitic acid and the Cd atoms. The connectivity between the acid and the Cd dimers are shown in Figure 5b. Of the four carboxylic acid groups, three form C−O−Cd bonds through all the oxygen atoms while the fourth one has one terminal C−O bond. Two of the carboxylate group has bidendate connectivity and the other two have monodendate linkage with Cd atoms. In addition, one of the oxygen atoms, O(4), links Cd(1) and Cd(2) atoms through a three-coordinate connection. The C−O bond distances are in the range 1.246(5)−1.269(5) Å (av. 1.258 Å) and O−C−O bond angles have an average value of 124.1°. These values are in the range expected for this type of bonding. The planar aromatic C−C and the terminal C−C

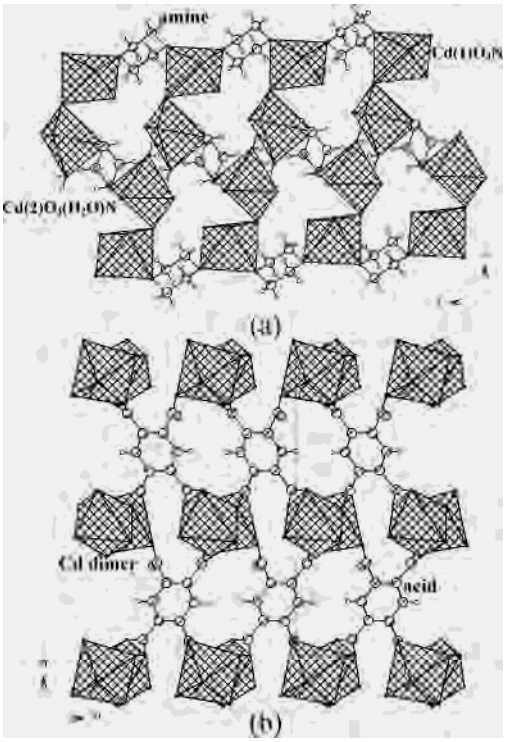

Figure 6. (a) Connectivity between the Cd dimers and the piperazine molecule in the *ac* plane. Note that the connectivity gives rise to a two-dimensional layer. The acid molecules are omitted for clarity. (b) Connectivity between the Cd dimers and the pyromellitic acid in the *ab* plane. The bound piperazine molecules are omitted for clarity.

bond distances are also in the range expected. Bond valence sum calculations[17] clearly indicate that the valence states of the Cd, C, and O atoms as +2, +4 and −2, respectively.

The structure of **II** consists of linkages involving the Cd dimers and the amine and acid molecules. The connectivity between the Cd dimers and the piperazine molecule gives rise to a two-dimensional layer in the *ac* plane (Figure 6a). Similarly, the connectivity between the Cd dimers and the acid also gives rise to two-dimensional structure in the *ab* plane (Figure 6b). The view of the structure along the *bc* plane is shown in Figure 7. As can be seen, the connectivity involving the acid and the piperazine molecule along with the Cd dimers gives rise to large elliptical channels involving four pyromellitate, two piperazine molecules, and six Cd dimers. The other piperazine molecule projects into the channels from the Cd center. This piperazine molecule may be amenable for chemical manipulation. Such functionalized channels have been reported recently in a Nd−oxalate three-dimensional frameworks.[18] Medium-strength hydrogen-bond interactions have been observed involving the hydrogen atoms of the water and the piperazine molecule with the oxygen atoms. The important hydrogen-bond interactions have been listed in Table 4.

Spectroscopic Investigations. The diffusive reflectance UV−vis spectra for polymers **I** and **II** have been carried out and are shown in Figure 8. The spectra show broad maxima at 310 nm for **I** and **II** with a shoulder at 260 nm.

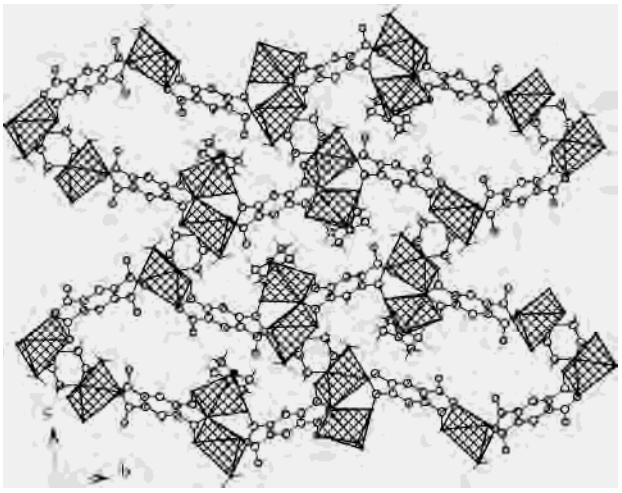

Figure 7. Structure of $[Cd_4(H_2O)_2(C_{10}H_2O_8)_2(C_4N_2H_8)_3]_\infty$, **II**, in the *bc* plane. Note that one of the bound piperazine molecule projects into the channels.

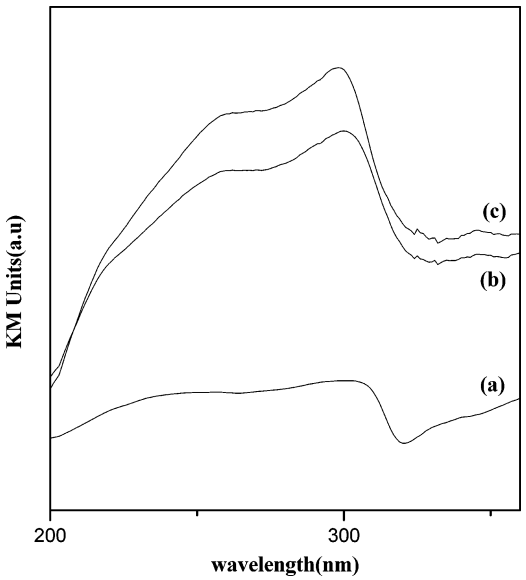

Figure 8. Diffuse reflectance UV−vis spectra for (a) the BTEC acid, (b) **I**, and (c) **II**.

The acid, BTEC, showed a maximum around 300 nm. This shift in the energy must be related to the bonding of the acid with the metal ions and may originate from the n → π^* transition with the n orbitals (HOMO located on the oxygen atoms of the carboxylate groups) being perturbed by the M^{2+} ions in the polymer. In addition, the absorption intensity of **I** and **II** is much higher than that of the acid. The significant increase in absorption intensity may be attributed to the involvement of the charge-transfer transitions from the O atoms of the acid ligands to the empty 4s orbitals of the M^{2+} ions. Both the compounds show photoluminescence (Figure 9). The emission spectra monitored at the excitation wavelength of 340 nm, shows a single maxima around 380 and 410 nm, respectively, for **I** and **II**. A similar emission band has also been observed in other zinc-organic polymer compounds.[19] The photoluminescence exhibited by the

(18) Vaidhyanathan, R.; Natarajan, S.; Rao, C. N. R. *Inorg. Chem.* **2002**, *41*, 4496.

(19) Chen, W.; Wang, J. Y.; Chen, C.; Yue, Q.; Yuan, H. M.; Chen, J. S.; Wang, S. N. *Inorg. Chem.* **2003**, *42*, 944.

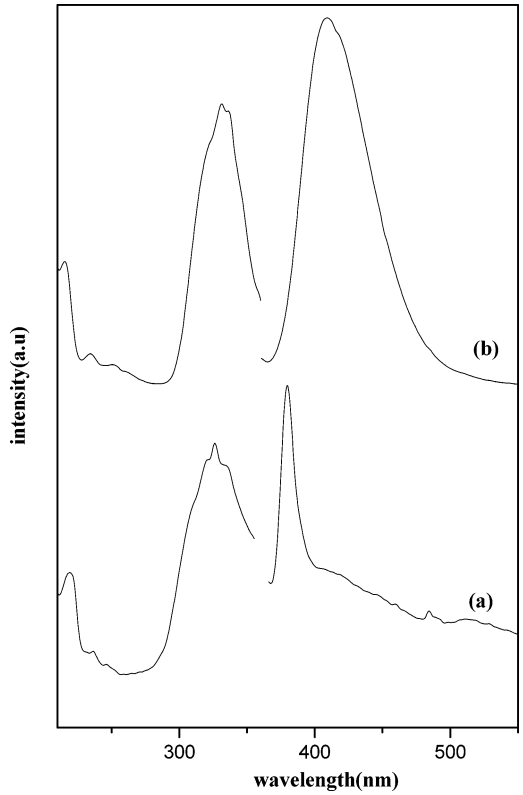

Figure 9. Solid-state photoluminescent spectra for (a) **I** and (b) **II**.

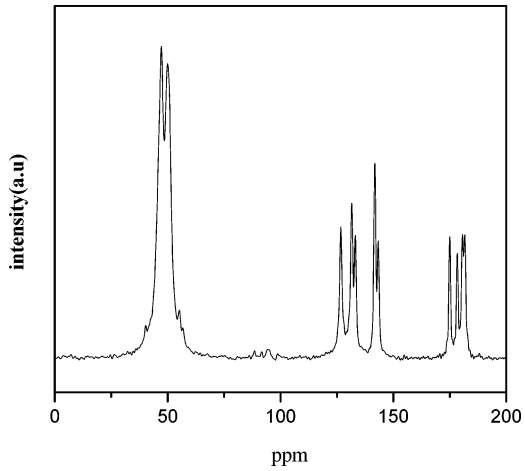

Figure 10. Solid-state ^{13}C MAS NMR spectra for **II**.

present compounds may be attributed to the ligand-to-metal-charge-transfer (LCMT). The strongest excitation peaks for both the polymers is around 330 nm. The excitation peaks of the polymer appear to be coincident, in peak position, with the threshold of the UV−vis absorption band of the polymer.

The MAS NMR spectra for both compounds appear to be similar, and we give the ^{13}C MAS NMR spectra for **II** in Figure 10. The ^{13}C MAS NMR, as expected, show typical signals.[20] For **I**, the signals are as follows: 41.233 and 48.443 ppm (CH_2-NH_2-piperazine); 121.988 ppm ($CH_{aromatic}$ unsubstituted, BTEC acid); 130.414, 134.338, 137.288, and 142.755 ppm ($C_{aromatic}$ with substitution, BTEC acid); 174.746, 180.958, and 182.313 ppm (COO group). For **II**, the peaks positions are as follows: 47.230 and 49.947 ppm (CH_2-NH_2-piperazine); 126.73 ppm ($CH_{aromatic}$ unsubstituted, BTEC acid); 131.590, 133.143, 141.819, and 143.296 ppm ($C_{aromatic}$ substituted, BTEC acid); 174.994, 178.338, 180.64, and 181.67 ppm (COO group). The observed differences could be due to the variations of the binding modes observed between the two compounds.

(20) Kemp, W. *Organic Spectroscopy*; Palgrave: New York, 1991.

Discussion

The compounds $\{[C_4N_2H_8][Zn_2(H_2O)(C_{10}H_2O_8)\}_\infty$, **I**, and $\{[C_4N_2H_8]_3[Cd_4(H_2O)_2(C_{10}H_2O_8)_2\}_\infty$, **II**, have been obtained as pure single-phase materials employing hydrothermal methods, and their structures were determined by single-crystal methods. Both **I** and **II** have three-dimensionally extended infinite coordination polymeric structures. Their structures involve linkages between the metal ions, the amine and the pyromellitic acid. The role of the amine molecules, in particular, is intriguing. A comparison of the pK_a values of the higher carboxylic acids of benzene, viz., trimesic and pyromellitic acid, gives an idea about the ease of removal of the proton from the carboxylic acid. (trimesic acid, pK_{a1} = 3.16, pK_{a2} = 3.98, pK_{a3} = 4.83; pyromellitic acid, pK_{a1} = 2.43, pK_{a2} = 3.13, pK_{a3} = 4.44, pK_{a4} = 5.61). From the pK_a values, it is clear that the initial removal of the proton from the pyromellitic acid appears to be easier but the removal of all the protons from the carboxylic acid might require an excess of base in the reaction mixture. In doing so, the additional base added during the mixing of the reactants might also lead to the amine molecules being linked to the metal ions. Such behavior of amine bonding to metal ions under high pH values has been observed earlier in some metal phosphate structures.[21] The reactions carried out under lower pH values predominantly gives rise to the known layered compound,[10] in addition to some uncharacterized powder.

Ligation by polyfunctional compounds such as 4,4′-bipyridine forming rigid networks is known to occur in oxalates and in other related compounds.[22,23] Ancillary ligation by water molecules has also been well established in many porous metal−organic frameworks.[24] In the present compounds, the ligation appears to be unique. Both **I** and **II** have terminal water molecules in addition to the ligation by the amine molecule. The amine molecule, which acts as a ligand in both compounds, connects two different metal centers. In a way, this helps in the building up of the three-dimensional structure. While in **II**, the connectivity between the amine and the metal ions give rise to a two-dimensional network (Figure 6a), in **I** the amine molecule connects just two metal centers only (Figure 2b). The ligation of the amine and water molecules observed here is somewhat similar to the cadmium succinate, $\{Cd_2(C_4H_4O_4)_2(C_4N_2H_8)(H_2O)_3\}_\infty$,

(21) Neeraj, S.; Natarajan, S.; Rao, C. N. R. *New J. Chem.* **1999**, *23*, 303.
(22) Li, H.; Kim, J.; Groy, T. L.; O'Keeffe, M.; Yaghi, O. M. *J. Am. Chem. Soc.* **2001**, *123*, 4867 and references therein.
(23) Lu, J. Y.; Lawandy, M. A.; Li, J. *Inorg. Chem.* **1999**, *38*, 2695.
(24) Pan, L.; Adams, K. M.; Hernandez, H. E.; Wang, X.; Zheng, C.; Hattoro, Y.; Kaneko, K. *J. Am. Chem. Soc.* **2003**, *125*, 3062 and references therein.

where the cadmium succinate layers are pillared by the amine molecule which connect the Cd centers through ancillary ligation.[25]

Though both **I** and **II** possess three-dimensional structure, there are distinct differences between the two structures. **I** contains distorted trigonal-bipyramidal $Zn(1)O_5N$ and tetrahedral $Zn(2)O_2(H_2O)N$ building units, and **II** has distorted octahedral $Cd(1)O_4N_2$ and $Cd(2)O_4(H_2O)N$ units. The connectivity of the amine molecules also presents an interesting comparison in the present structures. Thus, in **I**, the amine molecule appears to play the role of a simple ligand connecting two Zn atoms (Figure 2b). In **II**, however, the presence of two different amine molecules gives rise to a unique situation wherein one of the amine molecules appears to be projecting in to an extra-large elliptical channel in the *bc* plane. Though the nitrogen atoms of this amine molecule are part of the coordination requirement of the Cd atoms, it is likely that they may be amenable to chemical manipulations. Similar behavior of the piperazine molecules bound to metal centers and projecting into channels has also been observed in a three-dimensional cobalt pyromellitate.[7]

In **I** and **II**, the connectivity between the carboyxlate groups and the metal ions gives rise to two different situations. While both acid-1 and acid-2 in **I** are monodendate, in **II**, two of the carboxylate groups show bidendate connectivity (Figure 4 and Figure 6b). In **I**, acid-2 has four uncoordinated C−O bonds while acid-1 has all the carboxylate oxygen atoms connected to Zn. In **II**, only one uncoordinated C−O bond is observed. As can be noted, the terminal C−O bond distances, in both **I** and **II**, does not show any significant differences when compared to the bonded ones (Tables 2 and 3). The terminal oxygen atoms [C(11)−O(8) and C(20)−O(9) in **I** and C(21)−O(8) in **II**] appear to participate in medium-strength hydrogen bonding with both the water molecules bound to the metal ions and to the ligated amine molecules. It is likely that the hydrogen-bond interactions result in normal bond distances for the terminal C−O bond. In addition, C−H···O hydrogen-bond interactions between the carboxylate oxygen atoms and the piperazine molecule have been observed for both compounds. The C−H···O hydrogen bond and its role in crystal packing has been discussed in detail.[26] In **I** and **II**, the C···O distances are in the range 3.099(8)−3.446(7) Å and C−H···O bond angles are in the range 142−165° (Table 4). These are moderate hydrogen bonds and possibly contribute to the stability of this structure.

Conclusions

In summary, we have demonstrated the synthesis, structure, and photoluminescence properties of two new metal−organic polymers. In contrast to the previously reported structures, formed predominantly by carboxylic acids, the present compounds have ligation by the amine molecules. The secondary ligation of the amine molecules is interesting. This increases the structural diversity and variety of the known metal coordination polymers. Furthermore, the polymers can be excited directly to emit luminescence at room temperature. It is likely that more new materials can be prepared by careful choice of ligating amine molecules.

Acknowledgment. S.N. gratefully acknowledges the financial support from the Department of Science and Technology (DST), Government of India, through the award of a research grant.

Supporting Information Available: X-ray crystallographic file (CIF) for both compounds and figures showing % transmission vs wavenumber and % weight loss vs temperature of **I** and **II**. This material is available free of charge via the Internet at http://pubs.org.acs.org.

IC034836P

(25) Vaidhyanathan, R.; Natarajan, S.; Rao, C. N. R. *Inorg. Chem.* **2002**, *41*, 5226.

(26) Desiraju, G. R.*Crystal Engineering−The design of organic solids*; Elsevier: New York, 1989.